INFLUENCE OF PROCESSING ROUTES ON THE MORPHOLOGY AND PROPERTIES OF POLYMER/NANOFIBRILLATED CELLULOSE COMPOSITES

C. J. G. Plummer[a]*, S. Galland[a,b,c], F. Ansari[b,c], Y. Leterrier[a], P.-E. Bourban[a], L. A. Berglund[b,c], J.-A. E. Månson[a]

[a]*Laboratoire de Technologie des Composites et Polymères (LTC), Ecole Polytechnique Fédérale de Lausanne (EPFL), Station 12, CH-1015 Lausanne, Switzerland*
[b]*Department of Fiber and Polymer Technology, School of Chemical Science and Engineering, Royal Institute of Technology (KTH), 100 44 Stockholm, Sweden*
[c]*Wallenberg Wood Science Center, Royal Institute of Technology (KTH), SE-100 44 Stockholm, Sweden*
**christopher.plummer@epfl.ch*

Keywords: nanofibrillated cellulose, nanocomposites, processing, transmission electron microscopy.

Abstract
The morphology of polymer/nanofibrillated cellulose (NFC) composite sheets produced using different techniques and its influence on low strain stiffness were assessed by optical and transmission electron microscopy. Solvent processing led to relatively homogeneous NFC dispersions and significant reinforcement of the in-plane Young's modulus. The continuous cellular networks obtained by wet-comingling of PLA powder or latex with NFC also provided efficient and essentially scale-independent reinforcement, in spite of the extensive agglomeration of the NFC. However, the irreversible nature of these networks is incompatible with low pressure thermoplastic processing routes such as physical foaming, and while they may be broken up by e.g. extrusion, this led to substantial loss in reinforcement, particularly above T_g*, consistent with the observation of isolated low aspect ratio NFC aggregates in the extruded specimens.*

1. Introduction

The recent development of cost-effective routes for mass-producing nanofibrillar cellulose (NFC), based on enzymatic treatment of wood pulp followed by mechanical disintegration, has led to a regain in interest in the use of NFC to reinforce mechanical and barrier properties in conventional and bio-based plastics [1]. NFC is typically supplied as a dilute aqueous network of high aspect ratio, highly crystalline cellulose fibrils with diameters of 4 to 100 nm, an axial tensile strength of about 50 GPa and an axial tensile modulus widely assumed to be in the range 100-160 GPa, based e.g. on theoretical calculations and X-ray diffraction [2]. Experimental evidence from NFC "nanopaper" nevertheless suggests the effective tensile modulus of individual NFC fibrils at high concentrations to be significantly lower than this, owing to structural discontinuities [3]. Nanopaper is a dense, transparent NFC aggregate obtained by drying the aqueous gel to give a strongly hydrogen-bonded structure, a phenomenon known as "hornification" and which is irreversible under conventional processing conditions [4]. Obtaining homogeneous dispersions of NFC fibrils in plastics is

therefore challenging, particularly for hydrophobic matrices, because hornification renders melt compounding of thermoplastics with dried NFC ineffective, and final composite properties may be compromised by inadequate fiber-matrix interactions, aggregation and thermal degradation [3,5].

It is nevertheless possible to prepare hydrophobic polymer/NFC nanocomposites using solvent exchange with a suitable solvent/dispersant to obtain a wet NFC precursor containing a thermoplastic or polymerizable resin. After drying and thermal or photo-polymerization, if required, this method gives relatively homogeneous NFC dispersions in e.g. crosslinked epoxy and acrylate matrices, as well as thermoplastic polylactides (PLA) [2,5-7]. Significant aggregation may occur at high NFC contents, but this has to some extent been overcome by using chemical surface modification to reduce the hydrophilicity of the NFC [5]. An alternative is to introduce the polymer directly into the aqueous NFC gel in the form of finely dispersed fibers or particles prior to drying, a process known as "wet commingling" [8,9]. Nakagaito et al., for example, have described a process similar to papermaking in which aqueous NFC is mixed with PLA fibers with a diameter of 10 to 15 μm [8].

Optical and scanning electron microscopy (OM and SEM) are currently widely used to characterize polymer/NFC composites. While these are ideal for detecting coarse morphological features, OM, in particular, is of limited interest for probing the nanoscale dispersions assumed to be associated with e.g. solvent processing. Even so, there has been little use of transmission electron microscopy (TEM) to investigate NFC dispersions in plastics, in spite of its potentially greater resolution [10]. Given that characterization of the dispersions at all relevant length scales is likely to be key to understanding process-property-structure relationships in such materials, we have therefore used TEM to investigate NFC/polymer compounds prepared by compression molding of wet-comingled NFC and PLA latex or powder, twin-screw extrusion of the wet-comingled compounds and solvent-based impregnation of NFC with epoxy resin. The results are discussed in the light of literature data for the dependence of the tensile modulus on NFC content for the various types of composite.

2. Experimental

Epoxy/NFC composites were prepared as described elsewhere [6]. An aqueous 15-20 wt% NFC network, prepared by vacuum filtration of an NFC gel, was solvent exchanged with acetone and added to a solution of bisphenol-A diglycidyl ether (DGEBA, Sigma-Aldrich) resin and a polyetheramine (PEA, Huntsman) hardener. After drying to remove the acetone, the resulting precursor was cured at 80 °C for 3 hours and at 120 °C for a further 2 hours.

Homogenized wet-commingled PLA latex (particle diameters of 300 nm to 2 μm)/2 wt% NFC [9] was supplied as dry fluff by Innventia AB. After further vacuum drying overnight at 65 °C, the fluff was compression molded for 4 min at 150 °C with a bench-top press (Fontijne Holland, Netherlands) to give translucent films of about 0.3 mm in thickness. Wet-comingled ground PLA (PLA 8052D, NatureWorks LLC) powder (15 to 150 μm grain diameter)/5 wt% NFC (supplied as an aqueous 3.1 wt% NFC gel by Innventia AB) sheets were prepared as described by Boissard [11]. The dried sheets were compression molded for 10 min at 195 °C. Certain specimens were extruded at 180 °C under nitrogen using a twin-screw mini-extruder (DSM Micro 5 compounder, Netherlands) prior to compression molding.

Ruthenium tetroxide (RuO_4) staining was used to enhance the contrast between the polymer matrix and the NFC in the TEM images, and to stabilize the specimens in the electron beam.

30 to 50 nm thick transverse sections were prepared from the composites at room temperature using an ultramicrotome (Reichert-Jung Utracut E or Leica EM UC7) equipped with a diamond knife (Diatome) and picked up on 200 mesh copper TEM grids [10]. The sections were then exposed to RuO_4 vapor for 3 to 12 hours. All TEM imaging was carried out in bright field mode (Philips CM20 at 200 kV or FEI Tecnai Spirit at 80 kV).

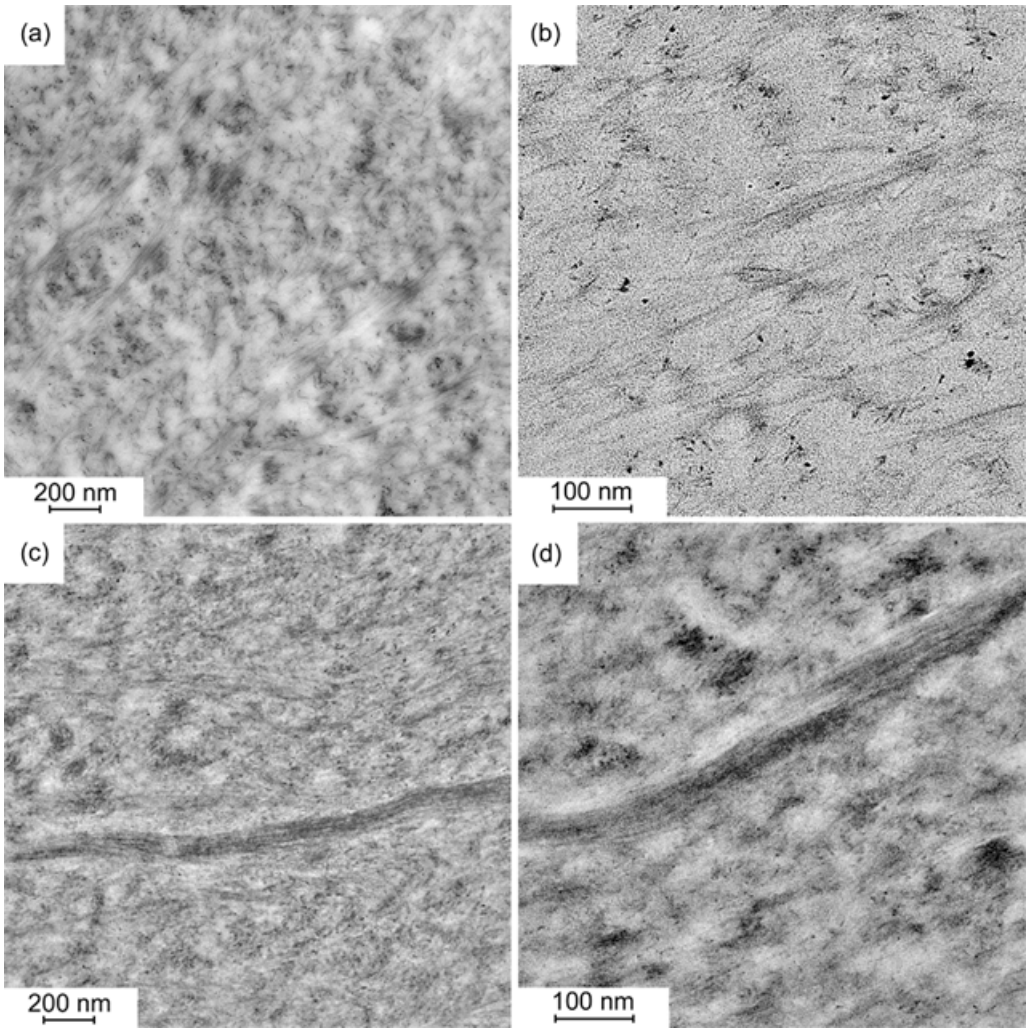

Figure 1. TEM images (negatives) of RuO_4 stained ultra-thin transverse sections from epoxy/15 vol% NFC (a,b) and epoxy/30 vol% NFC (c,d) films prepared by solvent processing [6].

3. Results and discussion

Figure 1 shows TEM micrographs of transverse sections from epoxy/15 vol% NFC and epoxy/30 vol% NFC, in which individual NFC fibrils with diameters of 4 to 5 nm are clearly visible, along with coarser bundles, these latter being more evident at the higher NFC content. The RuO_4 preferentially stained the epoxy matrix in this case, rather than the highly crystalline NFC, but negative images are shown for clarity in Figure 1, so that the NFC appears dark (images c and d in Figure 1 were also filtered to highlight fine structure). We were less successful in obtaining adequate contrast in NFC-based composites prepared in this way with a photo-polymerized acrylic matrix [7], which showed less tendency to absorb the RuO_4. On the other hand, as discussed elsewhere, RuO_4 staining gave acceptable results with solvent processed PLA/NFC films, where the PLA (or the amorphous regions of

semicrystalline PLA) was preferentially stained, although the definition in the images also depended on mass-thickness contrast induced by beam damage [10].

The trajectories of the individual NFC fibrils and fibril bundles were relatively straight at the scale of the micrographs in Figure 1. This may be inferred from both the fibrils whose axes were perpendicular to the plane of the sections, which appeared as dark spots, and the fibrils whose axes were closely aligned with the plane of the sections, which showed little apparent curvature over distances of up to 400 nm. The effective fibril aspect ratios were therefore at least 100, given a minimum fibril diameter of about 4 nm as estimated directly from the micrographs. This implies fiber efficiency factors, η_{LS}, greater than 0.9 in the Cox-Krenchel modified rule of mixtures (Equation 1) for discontinuous fiber reinforcement, assuming a fibril modulus, E_f, of 138 GPa, and a matrix shear modulus of 780 MPa [6,12]. On the other hand, η_{LS} is expected to be significantly lower for relatively coarse NFC bundles, e.g. that visible at the center of images c and d in Figure 1.

$$E_c \approx \eta_o \eta_{LS} \phi E_f + (1-\phi) E_m \quad (1)$$

Figure 1 also reflects the preferential alignment of the fibrils and fibril bundles with the plane of the specimens, which is further highlighted in Figure 2 by a lower magnification TEM image from epoxy/50 vol% NFC along with an image from atomic force microscopy (AFM, Veeco Multimode III) for comparison, in which a pronounced layered texture is visible. It follows that at high NFC concentrations, the solvent processing route led to roughly random in-plane fibril orientation, implying the orientation factor, η_o, in Equation 1 to be about 3/8 [12]. It is hence inferred that while the fibrils may to some extent have acted as independent reinforcing elements with a more isotropic orientation distribution at low concentrations, for which they were observed to be relatively well dispersed, the trend was towards a nanopaper-like structure as the concentration increased. Similar conclusions were reached from TEM observations of solvent processed PLA/NFC films referred to above, which showed an orthotropic, mat-like arrangement of NFC fibrils and fibril bundles, rather than a random orientation of the fibrils in three-dimensions [10].

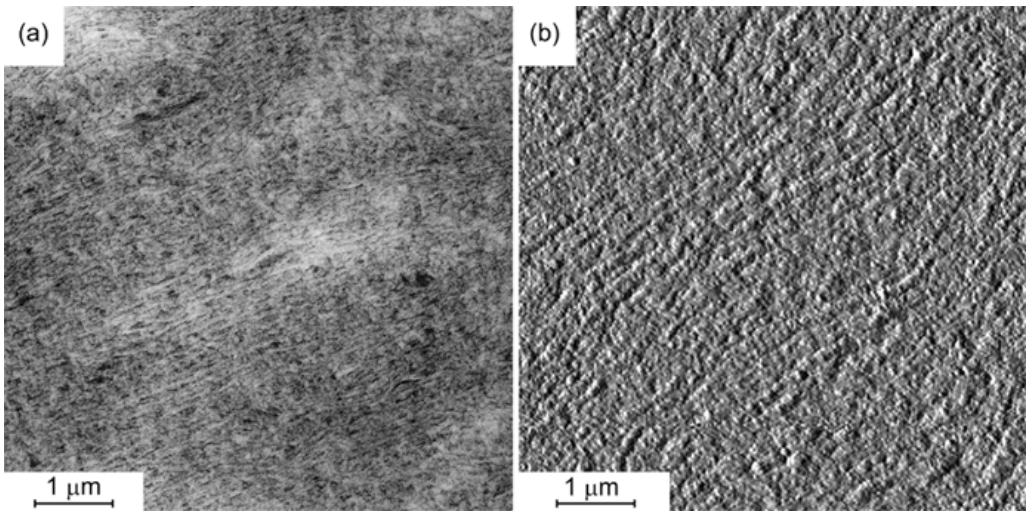

Figure 2. (a) TEM image of a RuO_4 stained ultra-thin transverse sections from an epoxy/50 vol% NFC film prepared by solvent processing [6] and (b) an AFM intermittent contact mode image (error signal) from the corresponding microtomed surface.

For both the ground powder and the latex PLA precursors, the wet-commingling process led to the formation of compact NFC aggregates between the precursor particles, as shown in Figure 3 for the PLA/NFC latex after drying and compression molding. In this latter case, the NFC was organized into bundles of 100 nm to 1 µm in diameter, arranged to form a network with a cell diameter of 300 nm to 5 µm, roughly consistent with the initial PLA particle diameters. As seen from Figure 3a, for the low NFC concentrations investigated here, the network was incomplete, in so far as the NFC bundles were not present at all the particle-particle interfaces. This resulted in local particle agglomerates that were essentially free of NFC, and a somewhat "ragged" network. However, as seen in Figure 3b, the NFC structure showed a high degree of continuity locally. There was also significant syneresis during compression molding, the PLA matrix being squeezed out from the NFC network, indicating this latter to have very limited capacity for flow and deformation, and implying efficient long range stress transfer throughout the structure, regardless of the state of the matrix [10].

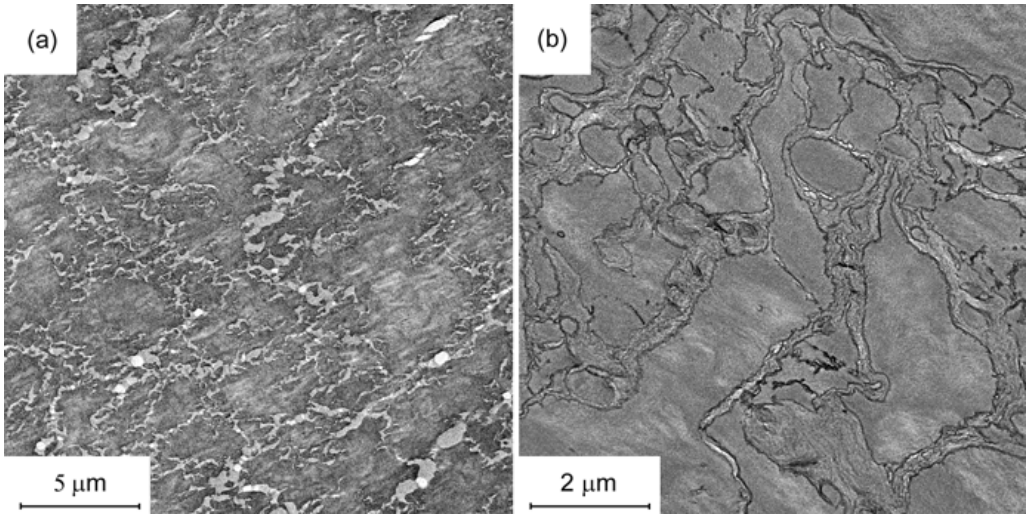

Figure 3. TEM micrographs at two different magnifications of an RuO_4 stained ultra-thin transverse section from a compression molded PLA/2 wt% NFC latex sheet [9,10].

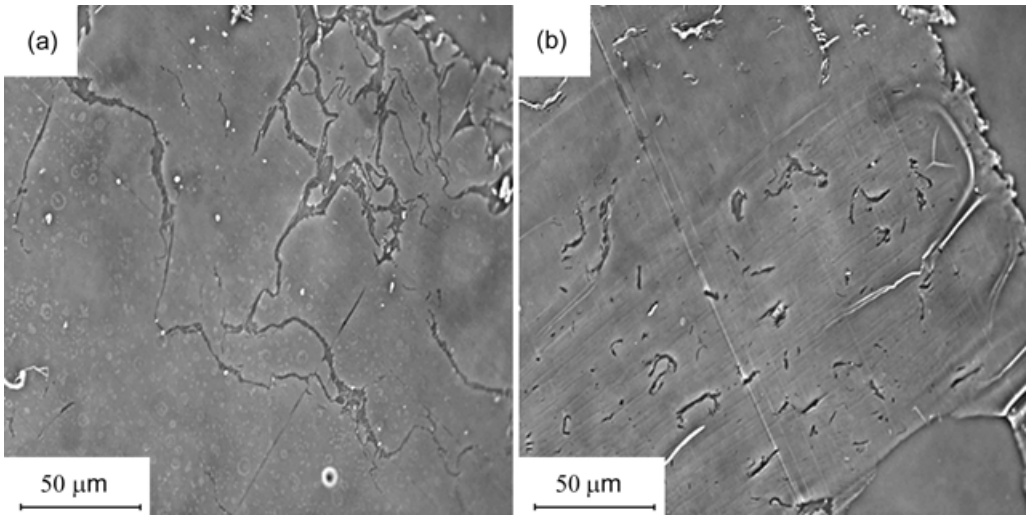

Figure 4. Optical micrographs (phase contrast) of transverse sections from wet-comingled ground PLA powder/5 wt% NFC: (a) hot-pressed (b) extruded and then hot-pressed [10].

In the case of the ground powder PLA precursors, the NFC aggregates again formed a continuous network, but the network cell diameter was in this case typically much greater than for the latex-based compounds, reflecting the precursor particle diameters of 15 to 150

μm, as shown in the OM micrograph in Figure 4a. Figure 4b shows the microstructure obtained after extrusion of the compound shown in Figure 4a, i.e. a roughly uniform dispersion of NFC bundles of 5 to 25 μm in length and 0.5 to 3 μm in diameter in the PLA matrix. Thus the shearing effect of the twin-screw extruder was sufficient to disrupt the continuous network structure, although it had little effect on the bundle thickness, resulting in coarse, low aspect ratio NFC aggregates, similar to those obtained from direct compounding of the matrix with dried NFC [11]. TEM of RuO_4-stained ultra-thin sections indicated all the NFC to be contained within these aggregates, with no NFC being present in the matrix-rich regions of either the compression moldings or the extrudates.

Figure 5 summarizes literature data for polymer/NFC composites prepared using the methods investigated here over a relatively wide range of compositions [6,8,9]. In all cases the limiting structure as the NFC content tends to 100 % was taken to be that of pure NFC nanopaper sheets with random in-plane fibril orientation, whose Young's moduli are reported to be in the range of 13 to 19 GPa [3]. Also shown in Figure 5a are the predictions of Equation 1 for NFC fibrils dispersed in the epoxy matrix, assuming η_o = 3/8 and for various $\eta_{LS}E_f$, the value of 124 GPa corresponding to an idealized NFC fibril with E_f = 138 GPa [13] and an aspect ratio of 100. Hence, while the experimental composite moduli for the solvent processed epoxy/NFC composites approached those predicted for an ideal dispersion at low NFC contents, the apparent fiber efficiency fell off markedly as the NFC content increased, an effect that may be attributed not only to increased aggregation of the fibrils but also to a reduced effective fiber modulus, as has been extensively discussed elsewhere in the context of the observed moduli for pure NFC nanopaper [3,6].

In the case of the wet-commingled compounds, the observation that the NFC forms relatively coarse aggregates at the interfaces between individual PLA particles during drying implies the formation of a network whose network strands are comparable in structure and hence in mechanical properties to those of the NFC nanopaper, regardless of the NFC content. The consistency between the data for the room temperature tensile modulus for the latex (particles of up to 2 μm in diameter) and much coarser fiber (10 to 15 μm in diameter) matrix precursors shown in Figure 5b also suggests reinforcement to be essentially scale independent [8,9]. Moreover, a simple linear rule of mixtures is roughly applicable over most of the composition range, not only at room temperature, but also at 90 °C, where the contribution of the PLA matrix to the composite modulus is negligible. This is consistent with reinforcement by a continuous rigid closed-cell foam made up of NFC nanopaper, as implied by the micrographs in Figure 3, bearing in mind that Figure 3 corresponds to a relatively low NFC content, so that the network was presumably less complete and less homogeneous than at higher NFC contents. This may account for the apparent discontinuity in slope of the data for the PLA latex/NFC composites at room temperature at around 20 wt% NFC, in which case this concentration presumably corresponds to the establishment of a fully connected NFC network.

The ground PLA powder-based wet-commingled composites were originally intended for physical foaming, but the NFC network was found to be sufficiently strong to suppress foam expansion of the plasticized matrix, reflecting an order of magnitude increase in the rubbery modulus in the presence of 5 wt% NFC (cf. the results in Figure 5b for the latex-based composites at 90 °C) [11]. This provided the rationale for using extrusion to reduce the network connectivity, as shown in Figure 4, but the resulting relatively low aspect ratio NFC agglomerates provided very little stiffness reinforcement in either the glassy or the rubbery state, consistent with predictions from the Halpin-Tsai equations [10,11], as well with results

obtained previously for polystyrene-clay nanocomposites prepared by sintering waterborne latexes, which were again characterized by a cellular arrangement of the clay nanoparticles after drying and compression molding [14].

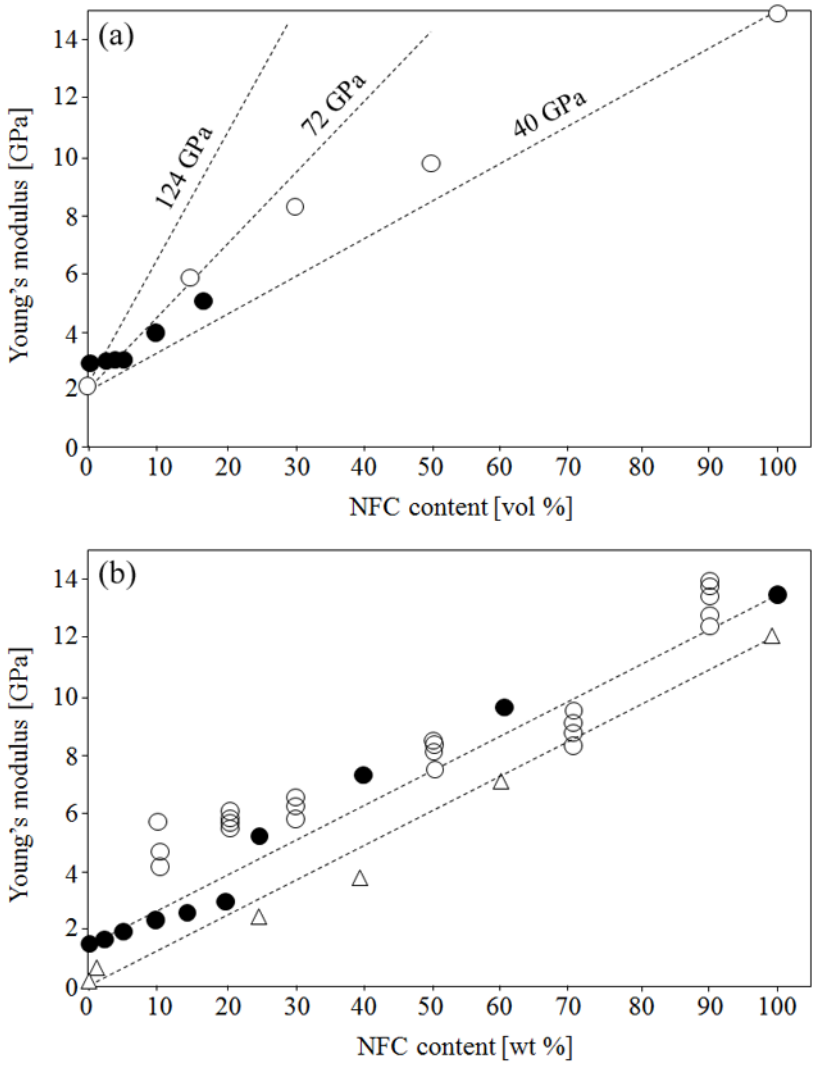

Figure 5. (a) Young's modulus as a function of NFC content in solvent processed films: open circles, epoxy/NFC [6], closed circles, PLA/NFC [5], along with the predictions of the Cox-Krenchel rule of mixtures (Equation 1) for the different values of $E_f\eta_{LS}$ indicated. (b) Young's modulus as a function of NFC content in wet-commingled composites: open circles, PLA fiber/NFC at room temperature [8], closed circles, PLA latex/NFC at room temperature, open triangles, PLA latex/NFC at 90 °C [9]. The hatched lines in (b) represent a simple rule of mixtures applied to the results for the PLA latex/NFC composites.

4. Conclusion

Wet-commingling is an effective means of reinforcing a polymer matrix with NFC, and has the advantage of versatility with regard to the choice of matrix, provided process temperatures are sufficiently low to avoid degradation of the NFC. On the other hand, effective reinforcement, particularly in the rubbery state, depends on establishing a continuous network of what is effectively NFC nanopaper, with the restrictions that: (i) the tensile modulus of nanopaper is significantly less than expected on the basis of the estimates for the modulus of the individual NFC fibrils; (ii) such a network cannot flow without loss of structural integrity, implying in turn that low pressure thermoplastic process routes are unsuited to this type of

composite, and that high pressure/high shear processes such as extrusion lead to a loss in reinforcement. Solvent processing is clearly less versatile in terms of the choice of matrix, but may be used to obtain close to ideal "nanodispersions" of the individual NFC fibrils at low NFC concentrations. In this case low strain reinforcement is consistent with classical micromechanical models for non-interacting inclusions. However, the reinforcing efficiency falls off with increasing concentration, the limiting modulus as the NFC content tends to 100 % being that of the pure nanopaper. It would hence be of interest to explore the effect of high shear processing on thermoplastics containing relatively low concentrations of well dispersed NFC fibrils, given that their low strain elastic response may be accounted for by simple micromechanical models that do not require connectivity between the reinforcing elements.

Acknowledgement

The authors wish to thank the Interdisciplinary Electron Microscopy Center (CIME) of the EPFL for its technical support.

References

[1] M. Henriksson, G. Henriksson, L. A. Berglund and T. Lindström. An environmentally friendly method for enzyme-assisted preparation of microfibrillated cellulose (MFC) nanofibers, *Euro Polym J*, 43(8):3434–3441, 2007.
[2] S. J. Eichhorn, A. Dufresne *et al.*, Review: current international research into cellulose nanofibers and nanocomposites, *J Mater Sci* 45:1–33, 2010.
[3] A. Kulachenko, T. Denoyelle, S. Galland and S. B. Lindström. Elastic properties of cellulose nanopaper, *Cellulose*, 19:793–807, 2012.
[4] G.V. Laivins and A. M. Scallan, The mechanism of hornification of wood pulps. *Proc 10th Fundamental Research Symposium*, PIRA International, Oxford, UK, pp 1235–1260, 1993.
[5] P. Tingaut , T. Zimmermann and F. Lopez-Suevos, Synthesis and characterization of bionanocomposites with tunable properties from poly(lactic acid) and acetylated microfibrillated cellulose, *Biomacromolecules*, 11:454–464, 2010.
[6] F. Ansari, S. Galland, M. Johansson, C. J. G. Plummer and L. A. Berglund, High cellulose nanofiber content in epoxy provides accelerated curing and moisture-stable biocomposites, to appear in *Composites A.*
[7] S. Galland, Y. Leterrier, T. Nardi, C. J. G. Plummer, J.-A. E. Månson and L. A. Berglund, UV-cured cellulose nanofiber composites with moisture durable oxygen barrier properties, to appear in *J Appl Polym Sci.*
[8] A. N. Nakagaito, A. Fujimura, T. Sakai, Y. Hama and H. Yano, Production of microfibrillated cellulose (MFC)-reinforced polylactic acid (PLA) nanocomposites from sheets obtained by a papermaking-like process, *Comp Sci Technol* 69:1293–1297, 2009.
[9] K. Larsson, M. Ankerfors and T. Lindström T, Properties of bionanocomposites made from poly(lactide) latex and microfibrillated cellulose, 2010, http://www.sustaincomp.com/Global/SustainComp/Published/Karolina%20Larsson%20-%20Properties%20of%20bionanocomposites.pdf (last consulted February 2014).
[10] C. J. G. Plummer, C. K. C. Choo, C. I. R. Boissard, P.-E. Bourban and J.-A. E. Månson, Morphological investigation of polylactide/microfibrillated cellulose composites, *Coll Polym Sci*, 291(9):2203–2211, 2013.
[11] C. I. R. Boissard, *Processing of sustainable cellular biocomposites*. PhD Thesis: Ecole Polytechnique Fédérale de Lausanne, 2012.
[12] H. Krenchel, *Fibre Reinforcement*, Akademisk Forlag, Copenhagen, 1964.
[13] I. Sakurada, Y. Nukushina and T. Ito, Experimental determination of the elastic modulus of crystalline regions in oriented polymers, *J Polym Sci*, 57:651–660, 1962.
[14] C. J. G. Plummer, R. Ruggerone, N. Negrete-Herrera, E. Bourgeat-Lami and J.-A. E Månson, Small strain mechanical properties of latex-based nanocomposite films. *Macromol Symp*, 294:1–10, 2010.